Experimental evaluation of a control system for active mass dampers consisting of a position controller and neural oscillator

T.Sasaki*[1], D. Iba[1] , J.Hongu[1] , M. Nakamura[1] and I. Moriwaki[1]

[1]Kyoto Institute of tech., Dept. of Mechanical Eng., Precision Manufacturing Lab., Goshokaido-cho, Sakyo-ku, Kyoto-shi, Kyoto, JAPAN

iba@ kit.ac.jp

Abstract. This paper shows experimental performance evaluation of a new control system for active mass dampers (AMDs). The proposed control system consists of a position controller and neural oscillator, and is designed for the solution of a stroke limitation problem of an auxiliary mass of the AMDs. The neural oscillator synchronizing with the response of a structure generates a signal, which is utilized for switching of motion direction of the auxiliary mass and for travel distances of the auxiliary mass. According to the generated signal, the position controller drives the auxiliary mass to the target values, and the reaction force resulting from the movement of the auxiliary mass is transmitted to the structure, and reduces the vibration amplitude of the structure. Our previous research results showed that the proposed system could reduce the vibration of the structure while the motion of auxiliary mass was suppressed within the restriction; however the control performance was evaluated numerically. In order to put the proposed system to practical use, the system should be evaluated experimentally. This paper starts by illustrating the relation among subsystems of the proposed system, and then, shows experimental responses of a structure model with the AMD excited by earthquakes on a shaker to confirm the validity of the system.

1. Introduction

Active mass dampers are widely used as anti-vibration devices for high-rise buildings to improve the livability. These systems have enough vibration reduction performance for swinging in the wind. However it faces the status quo that the system is forced to be shut down when large earthquakes occur [1]. It is because that there are two serious issues for the active mass dampers. One is the issue of robustness against parameter variation caused by the deformation and destruction of the structure, and the other is stroke constraint that depends on the location and motion of the active mass damper's auxiliary mass. To solve these problems, there has been considerable research on controllers based on the linear control theory and having various functions. As a result of the research, the revised controllers gave better results than that of the ordinary controllers, but the modifications have not been drastically improved and no prospect of actually using of the controllers has yet emerged.

On the other hand, neural oscillators, called central pattern generators (CPGs), have been extensively studied over the last few decades in the field of biological study [2-3]. The CPG can generate simple and rhythmic electrical signals capable of extending and retracting muscles [4], and be viewed as a significant component of the control system for animal locomotion. The most intriguing property of

the neural oscillators is the ability to harmonize with external periodic input. Because of this entrainment property to resonance, the neural oscillators can generate locomotion rhythm patterns in response to parameter changes of body (for example, a sprained leg) or changes in the environment and keep the appropriate and simple phase relation, such as the out-of-phase oscillations between a pair of left and right legs. Furthermore, mathematical models of the CPGs of animate beings have been studied. Matsuoka proposed a neuron model that is expressed by a pair of first order lag elements, i.e. simple enough to reproduce synchronization property. He also attempted to give mathematical proof of the condition for the generation of the vibration. These studies have been inspiring study of walking robots. Researchers who were interested in locomotive robots have studied to develop walking controllers using the pattern generators. Kimura et al. embedded the neuronal generator to a quadrupedal locomotion robot and developed the control system, which could walk on irregular ground without detailed data of the ground surface.

In contrast to these works on the active mass damper systems and locomotive robot systems, it seems that the relation between the both legs, which has stroke limitation and robust stability, is similar to the required relation between the structure and the auxiliary mass of the active mass damper for vibration reduction. Because of this background, a new control system for active mass dampers using the neural oscillator was proposed in our previous study [5]. The control system mimicking the motion of bipedal mammals is an incredibly simple system, which has the single neural oscillator synchronizing with acceleration response of structures. The travel distance and direction of the auxiliary mass of the active mass damper is determined by the output of the neural oscillator, and then, the auxiliary mass is transferred to the desired position by using a PID controller. This control system can generate the target displacement of the auxiliary mass from the structure's acceleration response; therefore, the system does not need the observation of fully state of the controlled object; in other words, it is unnecessary to design the observer. In addition, one of the purposes of the proposed system was to avoid the stroke restriction problem of the auxiliary mass during large earthquakes by restriction of the determined-desired value within the stroke limitation. It seemed that it was potentially possible to restrict the stroke of the auxiliary mass by the proposed. In fact, our previous study showed that the system suppressed the motion of the auxiliary mass during strong earthquakes in comparison with a linear controller [6]. However, no experimental study to evaluate the stroke restriction property of the proposed system had been done. In order to be utilized in practical application, the controller had to be analyzed by way of experiment.

The objective of this paper is to evaluate the vibration control performance and the stroke restriction property of the proposed system by an experimental apparatus equipped with a microcomputer with the proposed control algorithm installed. This paper starts by illustrating the relation among subsystems with reference to a block diagram, and explains the governing equations of the subsystems, then, shows experimental responses of the system with external input. Finally, the experimental results are examined and compared with the simulation results to evaluate the stroke restriction property.

2. The proposed system

The block diagram of the proposed active mass damper's system is shown in figure 1. In this system, the target model consists of a structure and a mass of the AMD. The acceleration response of the structure with the AMD to ground excitations, which is named as "Output 1" in this figure, is measured by an accelerometer on the structure. Next, a neural oscillator included in the neural system is synchronized with the acceleration response of the structure, and the desired value of the auxiliary mass can be determined by the oscillator's outputs. Finally, the PID controller drives the auxiliary mass to the desired value, and the inertial force of the auxiliary mass works to dissipate energy of the structural vibration. In this figure, "Output 2" is the relative displacement of the auxiliary mass of the active mass damper, which is the sensory feedback information for the positioning control. From the next subsection, the details of each block will be explained.

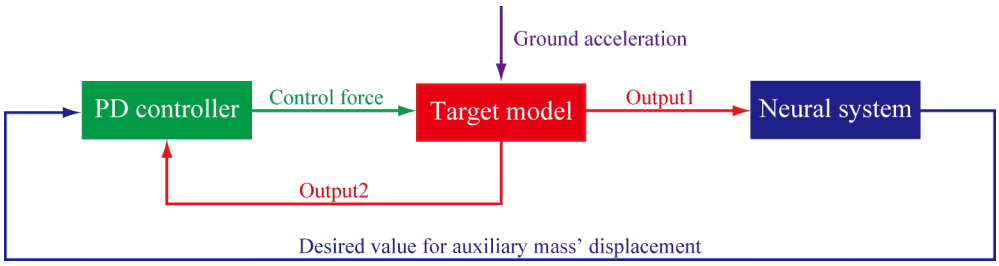

Figure 1. The block diagram of the proposed system

2.1. Target model

In this subsection, the target model for vibration control is explained. The target model, a single-degree-of-freedom structure with an active dynamic absorber, is shown in figure 2. The structure mass m_S is supported by the spring k_S and the damper c_S, which are connected in parallel. In this figure, x_S is the relative displacement of the structure mass and x_A is the relative displacement of the auxiliary mass. The mass m_A of the active mass damper on the top of the structure is driven by an actuator which generates the control force u. The equation of motion of the vibration model is obtained as equation (1). Where, the ground displacement is given z.

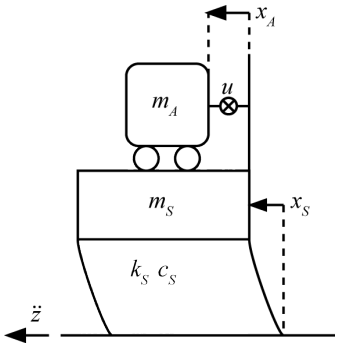

Figure 2. Overview of the target model

$$\begin{cases} m_S\ddot{x}_S + c_S\dot{x}_S + k_S x_S = -u - m_S(\ddot{x}_S + \ddot{z}) \\ m_A\ddot{x}_A + m_A\ddot{x}_S = u - m_A(\ddot{x}_S + \ddot{z}) \end{cases} \tag{1}$$

2.2. Neural system

In this subsection, the neural oscillator for the AMD system is explained. A Matsuoka's neural oscillator is used as the neural oscillator[7-8]. When absolute acceleration response of a structure is given to the neural oscillator as input, the mathematical model of the oscillator is obtained as in equation (2).

$$\begin{cases} \tau\dot{x}_e + x_e = -a\max(0, x_f) + s - bx'_e + \tau\varepsilon(\ddot{x}_S + \ddot{z}) \\ \tau\dot{x}_f + x_f = -a\max(0, x_e) + s - bx'_f - \tau\varepsilon(\ddot{x}_S + \ddot{z}) \\ T\dot{x}'_e + x'_e = \max(0, x_e) \\ T\dot{x}'_f + x'_f = \max(0, x_f) \end{cases} \tag{2}$$

This mathematical model contains two neural cell models and can establish sustained oscillation. Each cell model has two first-order lag systems to capture excitation and inhibition properties of the cell. Generally, this five parameters s, τ, T, b, a are determined by identification of a neuron, but the specified animate being is not considered in this study. The parameters are chosen by a design method to generate the oscillation with a natural frequency and amplitude desired. Here, ε means input gain to

the neural oscillator. According to the method, the natural frequency ω and the amplitude A of the oscillator can be expressed as following equations, which include the neural parameters.

$$\omega = \frac{0.212}{\tau}$$
$$A_0 = 0.612s \tag{3}$$

Where,

$$\begin{cases} \tau > 0 \\ s > 0 \\ T = 12\tau \\ b = a = \dfrac{(T-\tau)^2}{4T\tau} \end{cases} \tag{4}$$

This neural oscillator has to be synchronized with the response of structures to earthquakes. Assuming the response has mainly the component of the natural frequency, the neural oscillator should have the same natural frequency which the target structure has. Additionally, in this study, the amplitude of the oscillator is set to 1.

In addition, the synchronized neural oscillator can be considered that the output has the information of the structure response. Thus, in this study, the travel distance of the auxiliary mass and the driving timing are determined by the oscillator's state quantities. Here, an energy function using the oscillator's state quantities is introduced as

$$H = x_e'^2 + x_f'^2 \tag{5}$$

Using the oscillator's state quantities and the energy function, the desire value r (travel distance) of the auxiliary mass is obtained as

$$r = \begin{cases} -\alpha * \left| H - H_0 \right| & if\ x_e(t-\Delta t) < 0\ and\ x_e(t) > 0 \\ \alpha * \left| H - H_0 \right| & if\ x_f(t-\Delta t) < 0\ and\ x_f(t) > 0 \\ r(t-\Delta t) & else \end{cases} \tag{6}$$

Here, H_0 is the initial constant value of the energy function without the input, α is the conversion coefficient (output gain) from the oscillator energy to the travel distance of the auxiliary mass, and Δt is small time. In addition, when the desired value for the auxiliary mass is exceeded the limitation, the decided value by the neural system is replaced by the maximum value. In this paper, the stroke limitation of the auxiliary mass is described as

$$\left| r \right| \le R_{\max} \tag{7}$$

After the desired travel distance of the auxiliary mass is obtained, the position controller (in this study, PID controller) derives the auxiliary mass to the desired value.

2.3. Position controller

In this section, the position control is explained. The PID controller derives the auxiliary mass to the desired position, according to the information of the decided travel distance and direction by the neural system as shown in Figure 1. The P and I gains are the usual proportional and integral gains, but the D gain is not the usual differentiate gain but it works as the imaginary damper, which has negative sign to moderate the motion of the auxiliary mass. Here, K_P, K_I and K_D describe the proportional, integral and differential gain, respectively. The control force, which depends on the desired value r, is calculated as follow.

$$u = K_P(r - x_A) + K_I \int (r - x_A)\,dt - K_D \dot{x}_A \tag{8}$$

Here, the design method of the PID controller is explained. Generally, the PID controller as a position controller must be designed in consideration of the index about the quick response to the desired value. However, the control purpose of the proposed system is the energy dissipation by driving the auxiliary mass. Therefore, another index taking into account of energy dissipation is necessary for the PID gain design. The proposed design procedure is, firstly, the relationship between the P, I and D gains is restricted by reference to the critical damping of the vibration system, next, the driving path of the auxiliary mass depending on the P-gain is analytically solved from the motion equation without structures. Then, its ideal driving path for the auxiliary mass is introduced by assuming that the structure motion is swinging as a sinusoidal wave under sinusoidal excitation; i.e. its ideal driving path must be also a sinusoidal wave. Finally, the appropriate values of the P, I and D gains are determined by the value, which minimizes the inner product of the acceleration of the analytical solution x_A and the ideal path x'_A. According to this design method, the proportional gain P and the restricted I and D gains are obtained as follow.

$$\begin{cases} K_P = m_A k_{P,\max} \left(k_{P,\max} = \{k_P \left| \max(\cos\beta_A) \right.\}\right) \\ K_I = \dfrac{1}{3\sqrt{3}} m_A (k_{P,\max})^{3/2} \\ K_D = \sqrt{3} m_A (k_{P,\max})^{1/2} \end{cases} \tag{9}$$

Where, $k_W=K_W/m_A$, the cosine of the analytical solution x_A and the ideal path x'_A is obtained as follow.

$$\begin{aligned} \cos\beta_A &= \frac{\left\langle \ddot{x}_A, \ddot{x}'_A \right\rangle}{\left\| \ddot{x}_A \right\| \left\| \ddot{x}'_A \right\|} \\ &= \frac{\int_0^{\pi/\omega_n} \ddot{x}_A \ddot{x}'_A \, dt}{(\int_0^{\pi/\omega_n} \ddot{x}_A^2 \, dt)^{1/2} (\int_0^{\pi/\omega_n} \ddot{x}'^2_A \, dt)^{1/2}} \end{aligned} \tag{10}$$

3. Experimental apparatus

3.1. Vibration table

This subsection shows a vibration table system. Figure 3 shows the vibration table and its peripheral equipment. This vibration table system consists of a microcomputer (Arduino DUE) equipped with acceleration record of earthquakes, a laptop computer, which is for supply a start signal to the microcomputer, an amplifier and a shaking table. The microcomputer outputs the earthquake record with an appropriate sampling time to the amplifier, and the amplified signal is input to the shaking table to excite the structure. This system does not have any sensor for feedback, i.e. open-loop system. Therefore, the original earthquakes cannot be generated, because the generated motion on the shaking table is not controlled in the reproducible way.

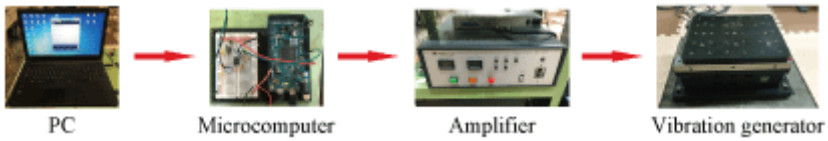

Figure 3. The photographic of the vibration generator and peripherals

3.2. Structure and active mass damper

Figure 4 shows the photograph of the developed structure equipped with the active mass damper system and figure 5 shows the outline of the equipment.

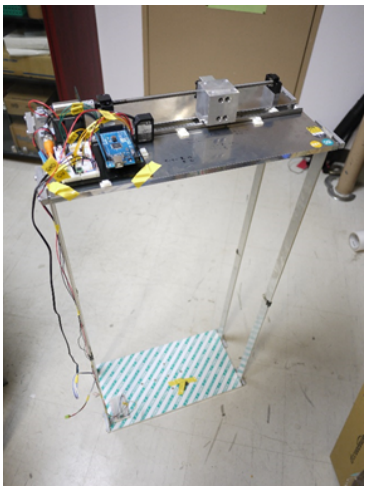

Figure 4. Photograph of apparatus

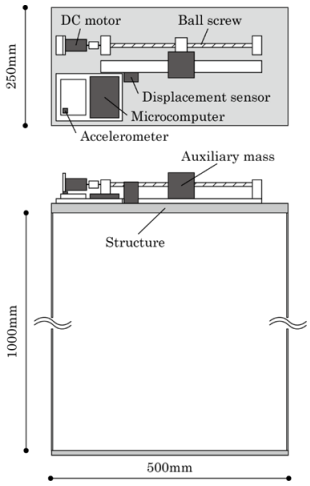

Figure 5. Outline of apparatus

The single-degree-of-freedom structure is made of duralumin and consists of four support plates, top and bottom plates. The active mass damper system is mounted on the top of the structure. The active dynamic absorber system consists of the auxiliary mass, which is made of duralumin and whose mass is 0.5 kg, a DC motor as an actuator to drive the mass, a ball screw to transfer rotation of the motor to translate motion, a microcomputer (Arduino Mega), in which the mathematical model of the neural oscillator and the algorithm for the target displacement of the mass using the oscillator output is embedded, a laser displacement sensor to measure the motion of the auxiliary mass, and acceleration sensors to measure the ground input and structure response. Table 1 shows the specifications of the structure and table 2 shows the specifications of the active mass damper system. The embedded the neural oscillator has the natural frequency at 1Hz to match the structure's natural frequency. Furthermore, the mass ratio of the auxiliary mass and the structure is 0.05. In addition, the maximum and minimum stroke of the auxiliary mass R_{max} is plus or minus 40 mm.

Table 1. Parameters of structure

Mass	10 kg
Natural frequency	6.22 rad/s (about 1 Hz)
Damping ratio	0.05

Table 2. Parameters of active mass damper

Auxiliary mass	0.5 kg
Ball screw	ϕ 8 mm, lead 4 mm
DC motor	4700 rpm, 17.3 mN·m, 12 V
Acceleration sensor	$\pm$2g, 600 mV/g, 5 V
Displacement sensor	$\pm$50 mm, 20 μ m, 10V
Microcomputer	Arduino MEGA2560

In addition, in order to put the active mass damper system to practical use, the control force generated by the above-mentioned PID controller should be transferred to the voltage applied to the DC motor with consideration of the inertia moment and transmission efficiency of the ball screw. In this paper, the following equation is used for the transformation.

$$V = \frac{1}{\mu} K_V K_M u \tag{11}$$

Where, K_M describes a coefficient in relation to the inertia moment, μ is the transmission efficiency and K_V describes the transformation coefficient from the control force to the voltage.

3.3. Friction force compensation

The retarding effect of friction on the motion of the active mass damper cannot be neglected in the actual system. The friction force acting on the system is considered as following equation.

$$\begin{cases} m_S \ddot{x}_S + c_S \dot{x}_S + k_S x_S - c_C \dfrac{\dot{x}_A}{|\dot{x}_A|} = -u - m_S \ddot{z} \\ m_A \ddot{x}_A + m_A \ddot{x}_S + c_C \dfrac{\dot{x}_A}{|\dot{x}_A|} = u - m_A \ddot{z} \end{cases} \tag{12}$$

Here, c_c is the coefficient of coulomb friction. For the PID gains design, the friction force is not considered in the equation of motion. Therefore, the actual displacement of the auxiliary mass driven by the designed PID controller is considered to not reach to the target displacement, or to not move in case of the small target displacement, because of the friction force. To avoid this situation, the compensation term F_f, which is related to the friction force, is introduced to the control force u as shown in the following equation.

$$u' = \begin{cases} u + F_f & if\ \dot{x}_a > 0 \\ u - F_f & if\ \dot{x}_a < 0 \end{cases}$$

However, the relative velocity $\dot{x}_a$ of the auxiliary mass is not measured in our system. Instead of using the relative velocity, a plus or minus sign of the desire value r is for switching. Thus,

$$u' = \begin{cases} u + F_f & if\ r > 0 \\ u - F_f & if\ r < 0 \end{cases} \tag{13}$$

3.4. Low-pass filter

The developed system has the acceleration sensor for measurement of structure response. However, the signal from the acceleration sensor is typically a combination of the structure response, sensor and environmental noise. In order to remove the effects of sensor and environmental noise, a low-pass filter is installed in the system. The low-pass filter we considered is a simple first order lag system, RC filter, which is obtained as the following equation.

$$\dot{y} + \frac{1}{CR} y = \frac{1}{CR} x \tag{14}$$

Where, x and y are the input and output voltage of the RC circuit. The cut-off frequency of this circuit is obtained as

$$f_c = \frac{1}{2\pi CR} \tag{15}$$

This filter is realized as a digital filter in the microcomputer.

$$y[n] = a_f y[n-1] + (1 - a_f) x[n] \tag{16}$$

Where,

$$a_f = \frac{CR}{CR + \Delta t}$$

and Δt is the sampling time of the microcomputer. The sampled acceleration response is the input to the filter as x and y is the output of the filter.

The low pass filter has a time delay. If the cut-off frequency was set to near the natural frequency of the structure model, and the phase delay of the filter would have a significant influence on the input to the neural oscillator. A small time delay would be preferred to improve the performance of the vibration reduction.

4. Results of shaking table test

In this section, we evaluate the vibration reduction performance and the stroke restriction property of the proposed system by the developed experimental apparatus equipped with the microcomputer with the proposed control algorithm installed. Table 3 shows the parameters of the neural system in the proposed system, and table 4 shows the parameters of the position control system we used in the test.

Table 3. Parameters of neural system

Parameters	Value
τ	0.0341
T	0.409
b	2.52
a	2.52
s	1.634
ε	15
α	0.8
H_0	0.2367

Table 4. Parameters of position control system

Parameters	Value
K_P	13
K_I	13
K_D	0
K_V	0.267
K_M	10
F_f	1.0
a_f	0.9

4.1. Evaluation of vibration control performance

Firstly, we evaluate the vibration control performance of the proposed system by experiment. Figure 6 (a) and (b) show the ground acceleration input to the structure model. El Centro NS, whose magnitude and time are appropriately modified for resonance, was used as the earthquake input. However, it can be seen in the figure 6(a)(b) that the measured acceleration is not identical to the original earthquake wave, because the shaking table was driven by the open-loop control system. The data (a) (black line) is for the structure without control, and the data (b) (red line) is for the structure with the proposed control system.

Figure 6(c)(d) show the acceleration responses of the structure without and with control. (c) is the structure's response without control (black line), and (d) is the response with the control system (red line). The convergence speed of the structure's acceleration response controlled by the proposed system was high, in other words, the transient response performance was improved. On the other hand, the acceleration response of the structure with the proposed controller is noisy data. Probably, the noise was generated by the motion of the ball screw and DC motor. We should have to look for ways to reduce noise near future.

Figure 7 shows the frequency response of the system with/without controller. In the figure, the black solid line is the resonance curve without controller and the red solid line is that of the structure

with the proposed control system. It appears that the peak at the resonance frequency was drastically reduced.

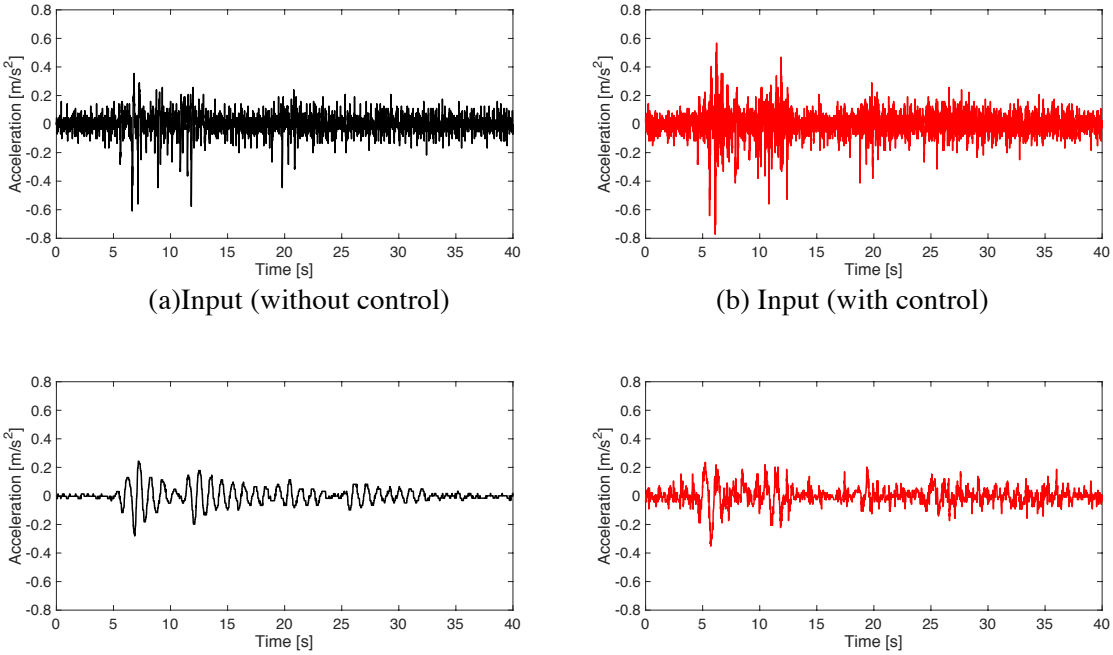

(a)Input (without control) (b) Input (with control)

(c)Output (without control) (d)Output (with control)

Figure 6. Input and output of structure with/without control

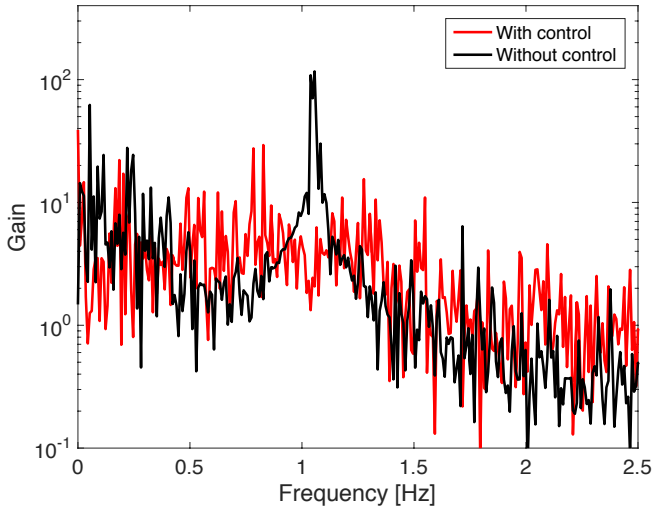

Figure 7. Resonance curves with/without control

4.2. Motion of the auxiliary mass and stroke constraint

In this subsection, we shall first verify through experiments that the position control system is able to achieve tracking performance to the ideal displacement path of the auxiliary mass. Figure 8 shows the target value generated by the neural system and the motion of the auxiliary mass driven by the DC motor and ball screw. The gray solid line is the target value for the auxiliary mass, and the blue solid line is the relative displacement of the mass. It appears that the auxiliary mass could move a little behind for the target value. However, it can be seen in this figure that the measured displacement data

of the auxiliary mass has overshoot phenomenon in the response. A possible reason is that the displacement measured by the laser displacement sensor has spikes in the data, the PD gain of the position controller is a bit high or the friction compensator is not accurate enough to cancel the friction force. We should have to improve the position control system for the stroke restriction problem near future.

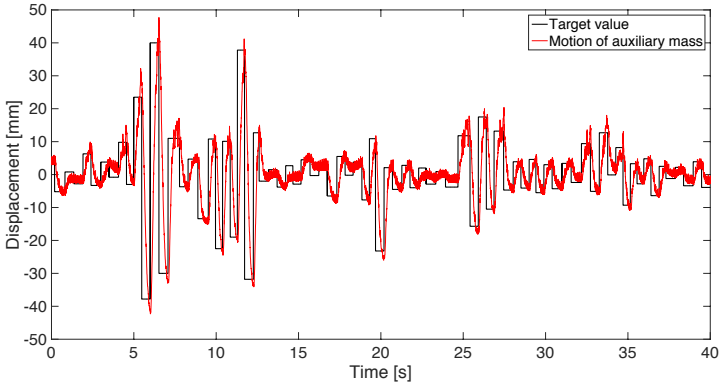

Figure 8. Target value and displacement of the auxiliary mass

Next, we evaluated the stroke restriction property of the proposed system. The double amplitude size earthquake was input to the structure, and the acceleration responses of the structure and the relative displacement of the auxiliary mass were measured during the ground shaking. The max-min stroke of the auxiliary mass is 40 mm.

Figure 9 (a) and (b) show the ground acceleration input to the structure model, whose amplitude are double compared with that of the abovementioned experiment. The black line (a) is the input to the structure without control and the red line (b) is the input to the structure with our controller. Figure 9 (c) and (d) show the acceleration responses of the structure with and without control. The response of the controlled structure (red line) differs very little from the response of the non-controlled structure (black line) compared with the small earthquake case.

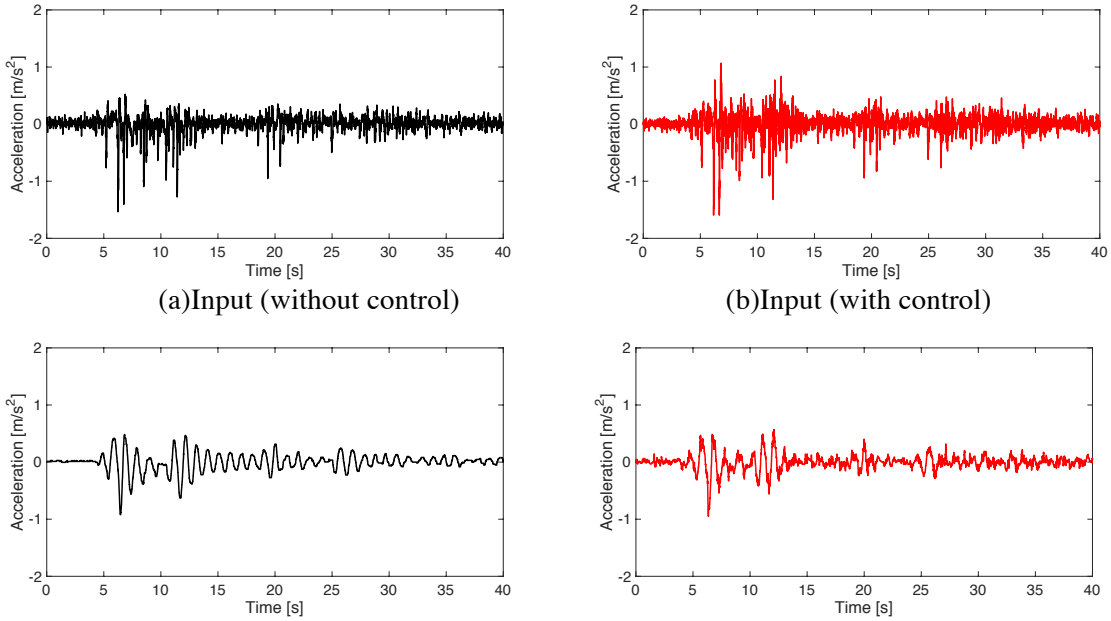

(a)Input (without control) (b)Input (with control)

(c)Output (without control) (d)Output (with control)

Figure 9. Input and output of structure with/without control (in case of large amplitude)

Figure 10 shows the resonance curves of the system with/without controller. In the figure, the black solid line is the resonance curve without controller and the red solid line is that of the structure with the proposed control system. It appears that the vibration reduction performance is not enough compared with the case of small size earthquake.

Figure 11 shows the target value and the relative displacement of the auxiliary mass. Because the stroke was restricted within plus or minus 40 mm, the maximum or minimum target value was also plus or minus 40 mm. Moreover, the motion of the position-controlled auxiliary mass was almost in the limitation. Due to this restricted motion of the auxiliary mass, the control performance of the system was reduced as shown in figure 10, however, we would not need to stop the system, even if large earthquakes happen. In this figure, as can be seen, the motion of the auxiliary mass has the overshoot phenomenon, but this problem will be improved by modification of the position control system.

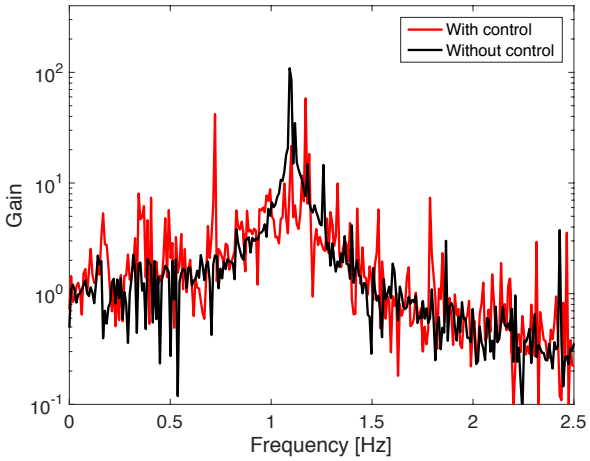

Figure 10. Resonance curves with/without control (in case of large amplitude)

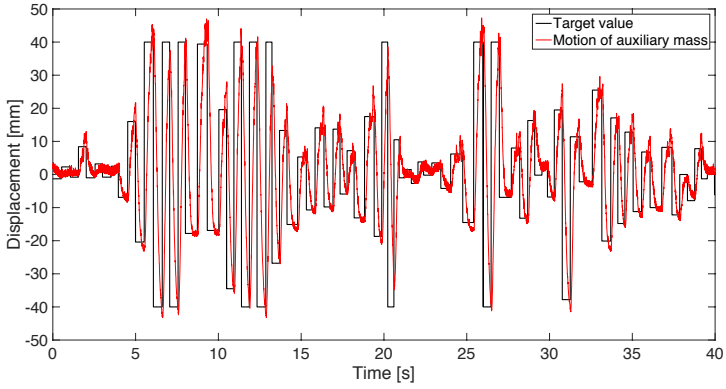

Figure 11. Restricted target value and displacement of the auxiliary mass

5. Conclusion

The objective of this paper was to evaluate the vibration control performance and the stroke restriction property of the proposed system by experiment. The proposed controlled system is a very simple control system, which is for the AMDs mimicking the motion of bipedal mammals and has a neural oscillator and a position controller. In the system, the auxiliary mass of the AMDs is operated to the desired position by the position controller, and therefore, it is easy to restrict the desired value within the limitation. However no study shows the control performance and the stroke restriction property of

the proposed system by experiment. Thus, in this paper, the proposed system was validated through experiments. First, the vibration control performance of the proposed system was evaluated. The experimental results showed that the acceleration response of the structure controlled by the proposed system was reduced. Second, the stroke restriction property of the proposed system was evaluated. The experimental results showed that the relative displacement of the auxiliary mass controlled by the proposed system was able to be within the limitation during large earthquake. Future work is to improve the position controller, which has a small time delay and efficient energy dissipation property.

Acknowledgement
The authors gratefully acknowledge the support by the support by the Ministry of Education, Culture, Sports, Science and Technology, Grant-in-Aid for Scientific Research (B), 15K05864

References

[1] Architectural Institute of Japan, *Active and Semiactive Control for Building –State of the Art-*, Maruyoshi Company (2006).
[2] Shik M L and Orlovsky G N, *Neurophysiology of locomotor automatism*, Physiol. Reviews, vol.56, pp. 465-501, (1976) .
[3] Taga G, "*Dynamical design of the brain and the body—Non-linear dynamical system and development of movement and perception*" (2002) .
[4] Kimura H, Fukuoka, Y, and Cohen A H, *Biologically inspired adaptive walking of a quadruped robot*, Philosophical Trans. of Royal Society in London, Vol.365, No.1850, pp.153-170, (2007) .
[5] Hongu J, Iba D, Nakamura M and Moriwaki I, "*Structural vibration control using an active mass damper operated by a combination system of a neural oscillator and position controller*" Transactions of the Japan Society of Mechanical Engineers, Vol. 81, No.825(2015), pp. 14-00668 (in Japanese) .
[6] Hongu J and Iba D, *Mutual synchronization between structure and central pattern generator*, Proceedings SPIE 8345, Sensors and Smart Structures Technologies for Civil, Mechanical, and Aerospace Systems 2012, 83451E (2012) .
[7] Matsuoka K, *Sustained oscillations generated by mutually inhibiting neurons with adaptation*, Biological Cybernetics 52, pp. 367-376, (1985) .
[8] Matsuoka K, *Mechanisms of frequency and pattern control in the neural rhythm generators*, Biological Cybernetics, Vol.56, pp.345-353, (1987) .